



Orbiting the Moons of Mars Including Higher Order Gravity Fields

Shaun Brown
University of Maryland

Abstract

This paper explores the orbit mechanics about the moons of Mars, Phobos and Deimos, in an extension of the restricted three body problem (R3BP). The dynamics model used includes the non-spherical gravity field of degree and order 4 for each moon. Periodic and quasi-periodic orbits are investigated using the surface of section technique. It has been found that orbits at distances greater than $r = 35\text{km}$ behave much like orbits with only central gravity terms. Periodic orbits are found when the equations of motion do not include S_{nm} terms in the gravity potential expansion. Orbits close to the moons with full gravity field were not found to be periodic but appear to stay in the vicinity for short periods of time and may be suitable for a mission that lands on the surface.

Introduction

The motivation for the studies in this paper stem from the speech President Bush gave January 14, 2004 announcing a new vision for U.S. space exploration, which included as the third goal returning to the Moon and establishing an extended human presence by 2020. After that goal is achieved, human missions to Mars and beyond will follow which make knowledge of the orbits about the moons of Mars important.

The two moons of Mars, Phobos and Deimos, are of interest to scientists, engineers and astrodynamacists. Some in the science community believe both moons are captured asteroids due to their tri-axial shape and apparent composition. Engineers would like to learn more about the moons for possible resource use and midway station for future Mars missions. Phobos is of interest to astrodynamacists for a few reasons. Firstly, the orbit of Phobos around Mars is faster than the rotation rate of Mars and tides in the body of Mars are causing the orbit of Phobos to shrink at a measurable rate, Shor [10]. Secondly, Phobos currently lies on or inside its Roche limit and could be torn apart soon depending on its internal strength, Dobrovolskis and Burns [12].

The present paper will further explore the dynamics of stable and periodic orbits around both Phobos and Deimos in the restricted three body problem (R3BP). Included will be the gravity field of degree and order 4 for Phobos from Chao and Rubincam [7] as well as for Deimos from Chao, Rubincam, and Thomas [6]. Earlier work has been published on orbiting the Martian moons by Jansson and Wiesel [1] where the dynamics model used included Mars and the moments of inertia for the Martian moons but ignored the moons eccentricity. Later work done by Wiesel [2] used a dynamics model that included Mars gravity and oblateness, the moons orbital eccentricity, and the moons moments of inertia. None of these previous dynamics models included the gravity field of degree and order 4 for each moon, which will be done here.

Dynamics and Methods

The aim of this paper will be to generate periodic orbits around the Martian moons and regions of stable orbits when the higher order gravity field of the moons is included. The analysis will be performed in the R3BP with the surface of section technique. In this section the underlying dynamics for the R3BP, higher-order gravity field and surface of section technique are derived.

Restricted 3-body Problem

The 3-body problem has been one of the most studied problems in astrodynamics since many three body systems are apparent in our own solar system, e.g. earth-moon-sun system. In general form the problem requires 18 integrals to solve yet only 10 are known. However, when assumptions to the problem are introduced particular solutions can be found. The assumptions are: the two massive bodies are in circular orbits in the x-

y plane around a common center of mass, the two primaries produce a gravitational influence on the third body, which has infinitesimal mass, but the third body has no influence on the primaries, the problem is scaled so that the total mass, distance between primaries, and mean motion of the primaries is unity. The problem for the motion of the infinitesimal body now requires 6 integrals, of which only 1 is known. The parameter μ is introduced as the mass ratio of the less massive body to the total mass. The system is then transformed into rotating coordinates so the primary masses remain on the x-axis. With these assumptions the general 3-body problem becomes the R3BP. The diagram for the R3BP is shown in Figure 1.

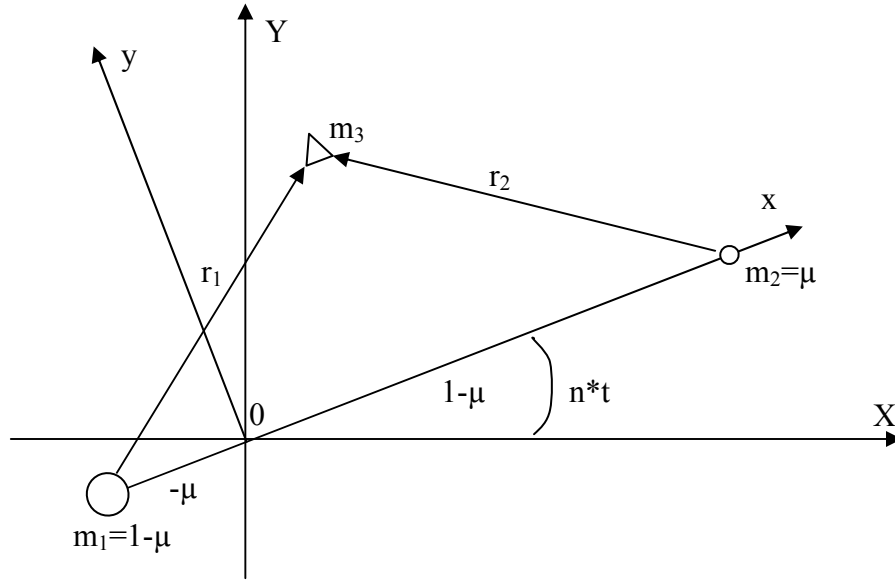


Figure 1 Geometry of the R3BP

The r_1 and r_2 vectors in Figure 1 are the vectors from the primary masses to the third mass, m_3 , which will be referred to as the particle throughout the paper. The origin of the coordinate system is the center of mass of the primaries, 0. The X-Y coordinate frame represents the fixed system while the x-y coordinate frame represents the rotating system. In both systems the Z and z axes are aligned and come out of the paper. The equations of motion (EOM) are derived from the diagram in Figure 1. They begin with distance from each primary to the particle in inertial coordinates.

$$\begin{aligned} r_1 &= \sqrt{(X - X_1)^2 + (Y - Y_1)^2 + (Z - Z_1)^2}, \\ r_2 &= \sqrt{(X - X_2)^2 + (Y - Y_2)^2 + (Z - Z_2)^2}. \end{aligned} \quad (1)$$

Then by using the inverse square law to represent the attraction between the primaries and transformation between the particle the EOM become.

$$\begin{aligned}
\ddot{X} &= -(1-\mu)\frac{(X-X_1)}{r_1^3} - \mu\frac{(X-X_2)}{r_2^3}, \\
\ddot{Y} &= -(1-\mu)\frac{(Y-Y_1)}{r_1^3} - \mu\frac{(Y-Y_2)}{r_2^3}, \\
\ddot{Z} &= -(1-\mu)\frac{(Z-Z_1)}{r_1^3} - \mu\frac{(Z-Z_2)}{r_2^3}.
\end{aligned} \tag{2}$$

The EOM then are transformed into rotating coordinates, i.e. (x,y,z), with the following equations.

$$\begin{aligned}
X &= x \cos t - y \sin t, \\
Y &= x \sin t + y \cos t, \\
Z &= z.
\end{aligned} \tag{3}$$

After the transformation in (3) the EOM from (2) become.

$$\begin{aligned}
\ddot{x} - 2\dot{y} &= \frac{\partial U}{\partial x}, \quad \ddot{y} + 2\dot{x} = \frac{\partial U}{\partial y}, \quad \ddot{z} = \frac{\partial U}{\partial z}, \\
\text{where} \\
U &= \frac{x^2 + y^2}{2} + \frac{1-\mu}{r_1} + \frac{\mu}{r_2}.
\end{aligned} \tag{4}$$

The EOM in (4) written out with the z included are:

$$\begin{aligned}
\ddot{x} - 2\dot{y} &= x - (1-\mu)\frac{(x+\mu)}{r_1^3} - \mu\frac{(x-1+\mu)}{r_2^3}, \\
\ddot{y} + 2\dot{x} &= y - (1-\mu)\frac{y}{r_1^3} - \mu\frac{y}{r_2^3} \\
\ddot{z} &= (1-\mu)\frac{z}{r_1^3} - \mu\frac{z}{r_2^3}.
\end{aligned} \tag{5}$$

where

$$\begin{aligned}
r_1 &= \sqrt{(x+\mu)^2 + y^2 + z^2}, \\
r_2 &= \sqrt{(x-1+\mu)^2 + y^2 + z^2}.
\end{aligned}$$

The only known integral for (5) is Jacobi's integral. Jacobi's integral is an energy type integral that can be found by multiplying each equation in (5) by the corresponding velocity term and add them to get

$$\dot{x}^2 + \dot{y}^2 + \dot{z}^2 = 2U - C = x^2 + y^2 + \frac{2(1-\mu)}{r_1} + \frac{2\mu}{r_2} - C. \quad (6)$$

The constant in (6) C is called Jacobi's constant. Of course, for a given set of initial conditions, Jacobi's constant stays constant for all time along the trajectory.

If $C > 0$, the region in which the trajectory of an object can travel in the R3BP is limited. In this case, motion can only occur where $v^2 \geq 0$. When the velocity terms in (6) are set to zero, surfaces of zero velocity can be found. These zero velocity surfaces limit the motion of an object to just one side of the surface. From (6) the motion of an object is limited to the region where

$$x^2 + y^2 + \frac{2(1-\mu)}{r_1} + \frac{2\mu}{r_2} > C \quad (7)$$

This restriction provides a limit on where the particle can not go, it provides little information about where the particle will go.

Non-Spherical Gravity Field

With the EOM derived in (4) the perturbations due to the non-spherical gravity potential of the Martian moons will now be included. The external gravity field potential must vanish when the Laplacian operator is applied, i.e. $\nabla^2 U = 0$. The solution is represented with spherical harmonics in spherical coordinates shown below [8]:

$$U(r, \phi, \lambda) = -\frac{\mu}{r} \left[1 + \sum_{n=1}^{\infty} \sum_{m=0}^n \left(\frac{R}{r} \right)^n (C_{nm} \cos(m\lambda) + S_{nm} \sin(m\lambda)) P_n^m(\sin(\phi)) \right], \quad (8)$$

where λ is longitude, ϕ is geocentric latitude, and R is the equatorial reference radius of the body. The equations for longitude and latitude in Cartesian coordinates are shown below:

$$\sin(\phi) = \frac{z}{r}, \quad (9)$$

$$\sin(\lambda) = \frac{y}{\sqrt{x^2 + y^2}}, \quad (10)$$

$$\cos(\lambda) = \frac{x}{\sqrt{x^2 + y^2}}, \quad (11)$$

where

$$r = \sqrt{x^2 + y^2 + z^2}. \quad (12)$$

P_{nm} is the associated Legendre polynomial of degree n and order m . C_{nm} and S_{nm} are harmonic coefficients and both the $P_{nm}(\sin(\varphi))\sin(m\lambda)$ and $P_{nm}(\sin(\varphi))\cos(m\lambda)$ terms are known as surface spherical harmonic functions.

The surface spherical harmonics are divided into three classes. When $m=0$ the harmonics are called zonal harmonics and have n zero crossings from pole to pole as well as being rotationally symmetric about the pole. When $n=m$ the harmonics are called sectorial and have no zero crossing from pole to pole, however have $2m$ zeros in longitude. When $n \neq m > 0$ the harmonics are called tesseral with $n-m$ zeros from pole to pole. Sometimes both the Legendre polynomial and harmonic coefficients are fully normalized. In that case the following normalization takes place:

$$\bar{P}_n^m(\sin(\phi)) = \sqrt{k(2n+1)} \frac{(n-m)!}{(n+m)!} P_n^m(\sin(\phi)), \quad (13)$$

$$\left\{ \begin{array}{l} \bar{C}_{nm} \\ \bar{S}_{nm} \end{array} \right\} = \sqrt{\frac{(n+m)!}{k(2n+1)(n-m)!}} \left\{ \begin{array}{l} C_{nm} \\ S_{nm} \end{array} \right\}, \quad (14)$$

where

$$k = \left\{ \begin{array}{ll} 1 & \text{for } m = 0 \\ 2 & \text{for } m \neq 0 \end{array} \right\}. \quad (15)$$

Table 1 Normalized Harmonic Coefficients for Phobos with Non-Normalized in Parentheses, with $R_0=11.12$ km, [7]

(n,m)	$C_{nm}(x10^{-2})$		$S_{nm}(x10^{-2})$	
(1,0)	0		0	
(1,1)	0		0	
(2,0)	-4.698	(-10.51 = - J_2)		
(2,1)	0.136	(0.176)	0.138	(0.178)
(2,2)	2.276	(1.469)	-0.0202	(-0.013)
(3,0)	0.293	(0.775 = - J_3)		
(3,1)	-0.309	(-0.473)	0.181	(0.277)
(3,2)	-0.847	(-0.289)	-0.0655	(-0.0224)
(3,3)	0.224	(0.0311)	-1.392	(-0.194)
(4,0)	0.762	(2.286 = - J_4)		
(4,1)	0.347	(0.330)	-0.0776	(-0.0698)
(4,2)	-0.288	(-0.0639)	-0.112	(-0.0252)
(4,3)	-0.280	(-0.0167)	0.337	(0.0201)
(4,4)	-0.120	(-0.00254)	-0.0622	(-0.00132)

Table 2 Normalized Harmonic Coefficients for Deimos with Non-Normalized in Parentheses, with Ro=6.25 km, [6]

(n,m)	$C_{nm}(x10^{-2})$		$S_{nm}(x10^{-2})$	
(1,0)	0		0	
(1,1)	0		0	
(2,0)	-4.827	(-10.79 = -J ₂)		
(2,1)	-0.0727	(-0.0939)	0.362	(0.468)
(2,2)	4.773	(3.081)	0.122	(0.0791)
(3,0)	0.970	(2.566 = - J ₃)		
(3,1)	1.430	(1.545)	0.0521	(0.0562)
(3,2)	-1.108	(-0.379)	-0.499	(-0.170)
(3,3)	-0.121	(-0.0168)	0.728	(0.101)
(4,0)	0.508	(1.524 = - J ₄)		
(4,1)	-0.663	(-0.629)	0.0257	(0.0244)
(4,2)	-0.520	(-0.116)	0.689	(0.154)
(4,3)	1.137	(0.0680)	-0.614	(-0.0367)
(4,4)	1.200	(0.0254)	-0.274	(-0.00579)

To get the acceleration on the particle from the potential function in (8), partial derivatives with respect to each variable along with partial derivatives of the spherical coordinates with respect to the Cartesian coordinates are needed to use the chain rule. This is shown in (16) through (18) below:

$$\ddot{x} = -\frac{\partial U}{\partial r} \frac{\partial r}{\partial x} - \frac{\partial U}{\partial \phi} \frac{\partial \phi}{\partial x} - \frac{\partial U}{\partial \lambda} \frac{\partial \lambda}{\partial x} \quad (16)$$

$$\ddot{y} = -\frac{\partial U}{\partial r} \frac{\partial r}{\partial y} - \frac{\partial U}{\partial \phi} \frac{\partial \phi}{\partial y} - \frac{\partial U}{\partial \lambda} \frac{\partial \lambda}{\partial y} \quad (17)$$

$$\ddot{z} = -\frac{\partial U}{\partial r} \frac{\partial r}{\partial z} - \frac{\partial U}{\partial \phi} \frac{\partial \phi}{\partial z} - \frac{\partial U}{\partial \lambda} \frac{\partial \lambda}{\partial z} \quad (18)$$

These partials are shown explicitly in (19) through (24) below:

$$\frac{\partial U}{\partial r} = \frac{\mu}{r^2} \left[1 + \sum_{n=2}^{\infty} \left[\frac{R}{r} \right]^n \sum_{m=0}^n (C_{nm} \cos(m\lambda) + S_{nm} \sin(m\lambda)) (n+1) P_n^m(\sin(\phi)) \right], \quad (19)$$

$$\frac{\partial U}{\partial \phi} = -\frac{\mu}{r} \sum_{n=2}^{\infty} \left[\frac{R}{r} \right]^n \sum_{m=0}^n (C_{nm} \cos(m\lambda) + S_{nm} \sin(m\lambda)) [P_n^{m+1}(\sin(\phi)) - m \tan(\phi) P_n^m(\sin(\phi))] \quad (20)$$

$$\frac{\partial U}{\partial \lambda} = -\frac{\mu}{r} \sum_{n=2}^{\infty} \left[\frac{R}{r} \right]^n \sum_{m=0}^n (S_{nm} \cos(m\lambda) - C_{nm} \sin(m\lambda)) m P_n^m(\sin(\phi)), \quad (21)$$

$$\frac{\partial r}{\partial x} = \frac{x}{r}, \quad \frac{\partial r}{\partial y} = \frac{y}{r}, \quad \frac{\partial r}{\partial z} = \frac{z}{r}, \quad (22)$$

$$\frac{\partial \lambda}{\partial x} = \frac{-y}{(x^2 + y^2)}, \quad \frac{\partial \lambda}{\partial y} = \frac{x}{(x^2 + y^2)}, \quad \frac{\partial \lambda}{\partial z} = 0, \quad (23)$$

$$\frac{\partial \phi}{\partial x} = \frac{-zx}{r^2 \sqrt{x^2 + y^2}}, \quad \frac{\partial \phi}{\partial y} = \frac{-zy}{r^2 \sqrt{x^2 + y^2}}, \quad \frac{\partial \phi}{\partial z} = \frac{r^2 - z^2}{r^2 \sqrt{x^2 + y^2}}. \quad (24)$$

The Legendre polynomials are computed with recursion formulae. Depending on whether the harmonic is zonal, sectorial or tesseral the computation for the Legendre polynomial are given by.

$$\text{For zonal, } m=0: P_n^0(\sin(\phi)) = \frac{1}{n} [(2n-1)\sin(\phi)P_{n-1}^0(\sin(\phi)) - (n-1)P_{n-2}^0(\sin(\phi))] \quad (25)$$

$$\text{For tesseral, } n \neq m \text{ and } m \leq n: P_n^m(\sin(\phi)) = P_{n-2}^m(\sin(\phi)) + (2n-1)\cos(\phi)P_{n-1}^{m-1}(\sin(\phi)) \quad (26)$$

$$\text{For sectorial, } m=n: P_n^m(\sin(\phi)) = (2n-1)\cos(\phi)P_{n-1}^{m-1}(\sin(\phi)) \quad (27)$$

$$\text{To get the recursion started both: } P_j^j(\sin(\phi)) = (-1)^j (2j-1)! (1 - \sin(\phi)^2)^{\frac{j}{2}} \quad (28)$$

$$\text{and } P_{j+1}^j(\sin(\phi)) = \sin(\phi)(2j+1)P_j^j(\sin(\phi)) \text{ are needed.} \quad (29)$$

Surface of Section

If motion is restricted to the x-y plane, the R3BP EOM shown in (4) have two degrees of freedom which means the phase space has four dimensions, i.e. x, y, \dot{x}, \dot{y} . Since there is one integral to the EOM in (4) shown in (6) the motion of the particle is constrained to move on a three-dimensional manifold (surface) in the four-dimensional space.

The surface of section technique introduces a surface S into the phase space where a second independent integral may be discovered. If a second quasi-integral exists, the intersection of the two-dimensional manifold may result in sets of closed curves, while chaotic trajectories show up as scattered points across section plane. The term quasi-integral is used, since it is impossible for numerical experiments to determine the

existence of a second integral. In fact, studies show that a second integral does not exist, (Moser 1955, Cushman 1970).

The surface of section technique is parameterized by Jacobi's constant (C) and the mass ratio μ . The criteria for the surface S is defined by either:

$$\dot{r}_1 = 0 \quad (30)$$

$$\text{or} \\ x\dot{x} + y\dot{y} = 0. \quad (31)$$

Equations (30) and (31) represent the condition for the orbit to be at a relative extremum [5]. To make a surface of section plot the EOM in (4) are integrated over a finite length of time and when the criterion in (31) is met the x and y values at that time are plotted in configuration space. Once the plot is generated the qualitative features of the orbits can be detected by recognizing the patterns, that is, observing whether the points appear to lie on a curve or not.

Results and Discussion

In the first section of results the trajectories were integrated with the R3BP using only central gravity terms. The results agreed with what was already known, which is there are both stable and periodic orbits that exist around both Martian moons [1,2]. Some of these periodic orbits are shown here for comparison with later results.

All the results in this section were attained by using the constants in Table 3.

Table 3 Constants for Mars, Phobos and Deimos

	Phobos	Deimos	Mars
GM parameter, km/s ²	7.158 x 10 ⁻⁴ [3]	9.8 x 10 ⁻⁵ [3]	42828.37 [3]
Mean Radius, km	11.1 ± 0.15 [4]	6.2 ± 0.18 [4]	3397 [8]
Mean Orbital Radius, km	9380 [8]	23460 [8]	-

The EOM in (4) for the R3BP are invariant under the transformation t goes to -t and y goes to -y. This identity allows symmetric periodic orbits to be found by searching for orbits that make perpendicular crossing of the Mars-moon axis (x-axis). These periodic orbits were found by integrating the EOM in (4) at a point near the moon on the x-axis with an initial velocity in the y-direction only. To ensure the orbit will be periodic, a search is performed for a starting velocity that will guarantee the subsequent crossing of the x-axis have velocities in y-direction only, i.e. perpendicular crossings of the x-axis. At very close distances from the moons the central term dominates and the orbital motion approaches the two-body periodic case. The above method seeks to continue the two-body periodic orbits into the R3BP. Figure 2 shows two periodic orbits around Phobos at two different radii with central gravity terms only.

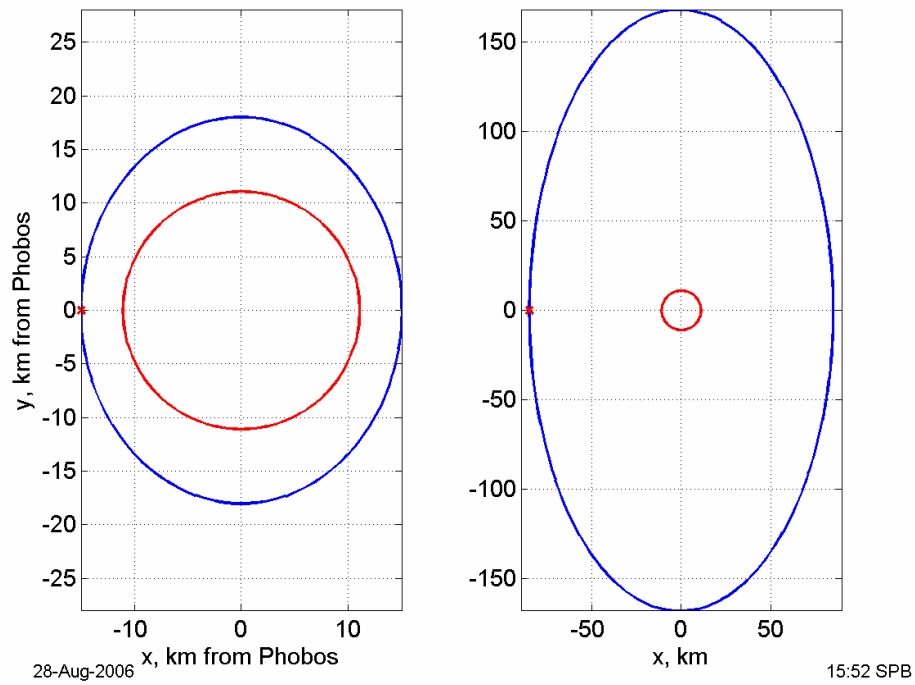


Figure 2 Periodic retrograde orbits around Phobos in the R3BP with radii of 15 km and 85 km

Periodic orbits were also found for Deimos at the same two radii. Figure 3 shows two periodic orbits with central gravity terms only.

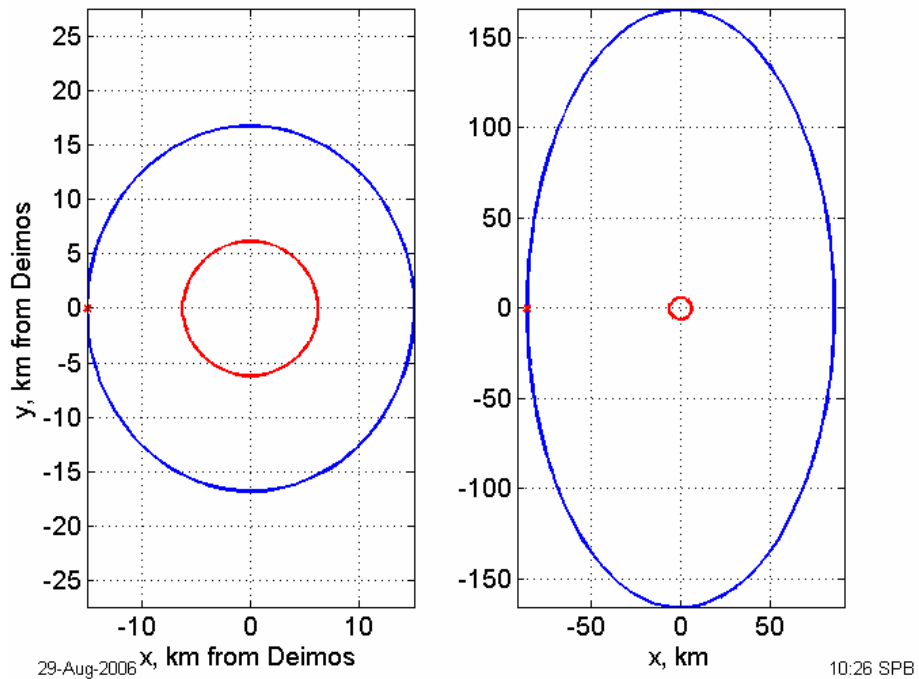


Figure 3 Periodic retrograde orbits around Deimos in the R3BP with radii of 15 km and 85 km

The characteristics of these central gravity orbits for Phobos and Deimos are summarized in Figure 4. The ratio of y-axis (R_{max}) to x-axis (R_{min}) for Phobos is nearly 2:1 for orbits up to very close distances. The period of Phobos orbits is as low as two hours for very close distances and up to Phobos orbital period by 60 km orbits. This period difference is because at distances above 60 km the gravity of Phobos has little affect and the particle is essentially in orbit around Mars. The maximum orbital velocity (V_{max}) with respect to Phobos throughout the altitude range is less than 55 m/s, which suggests maneuvering from one location to another on the moon, is not very expensive. Similar results are also shown for Deimos with and even lower V_{max} , i.e. $<10\text{m/s}$.

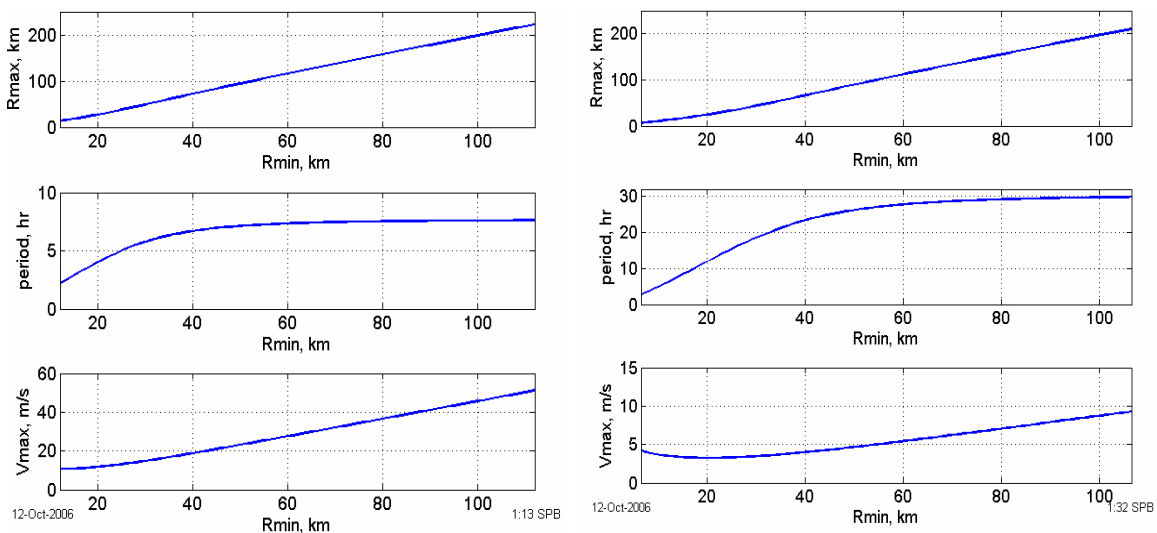
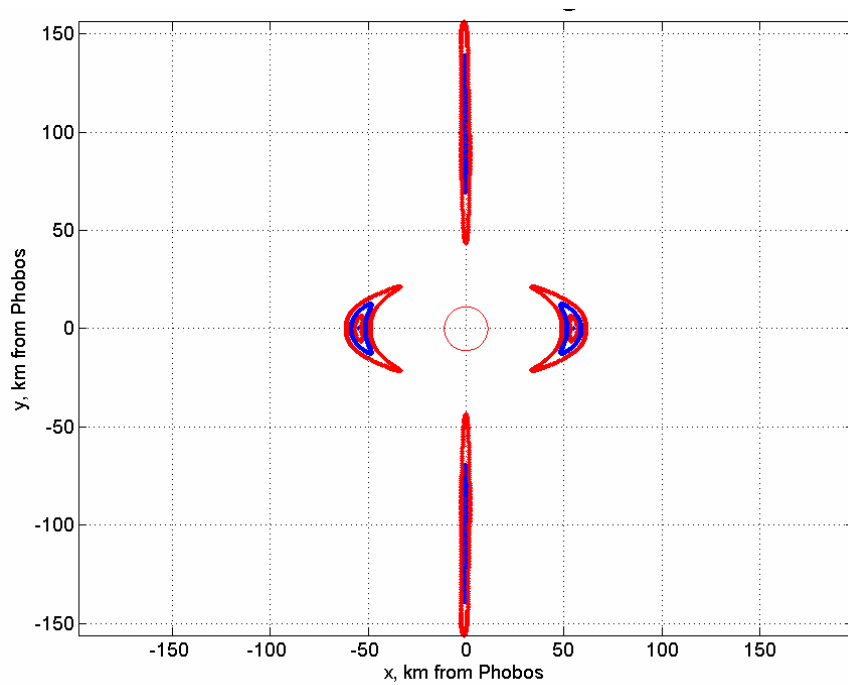


Figure 4 Orbital characteristics for Phobos (left) and Deimos (right) with only central gravity terms

With only central gravity terms periodic orbits can be found at any altitude above the surface of the moons. Direct orbits that did not collide with the moons could not be found when the same techniques as retrograde orbits are used. To understand the difference between direct and retrograde orbits first imagine a moon and Mars as a two-body problem where the angular momentum vector is determined by crossing the radius vector and the velocity vector. If the particle is orbiting a moon in a two-body sense the angle between the angular momentum vector of the particle and the angular momentum vector of the moon is the inclination. If the inclination is less than 90° then the orbit is said to be direct and over 90° is retrograde.

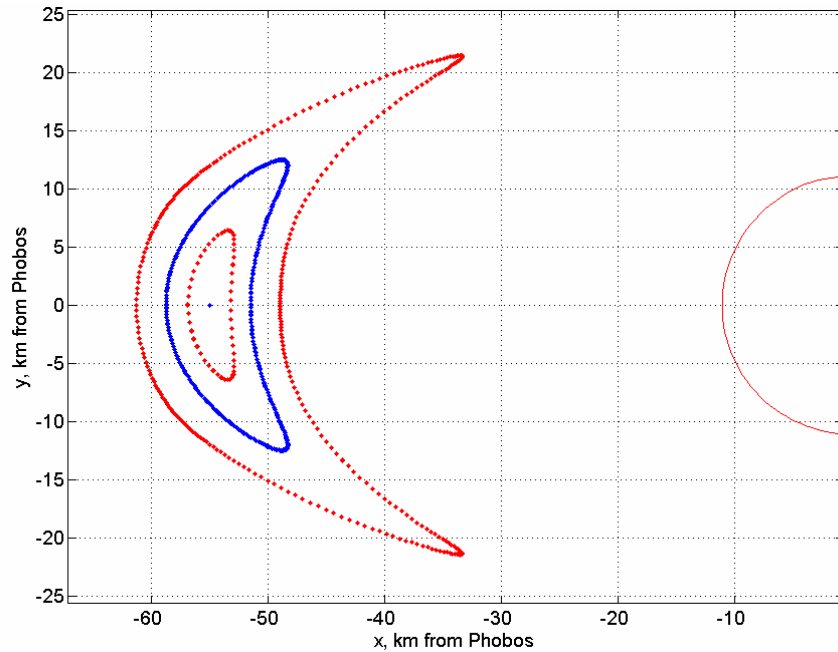
Stable orbits that are quasi-periodic can also be found by using the surface of section technique. Beginning with the value of Jacobi's constant for a periodic orbit then changing the initial location along the x-axis the new velocity in the y direction can be found to retain the same Jacobi's constant. This method will map out stable orbit regions around each of the moons as shown in Figure 5 and Figure 6.



29-Aug-2006

10:57 SPB

Figure 5a Surface of section for Phobos with $C = 2.99996559$



29-Aug-2006

10:57 SPB

Figure 5b Enlarged view of left side of Figure 5a

Figure 5 shows four stable orbits regions for Phobos, which are enclosed inside the curves. The very center blue dot at $r = 55$ km is the initial periodic orbit. The method used to create Figure 5 begins with that periodic orbit and changes the initial conditions such that the initial x-location is shifted on the x-axis and the y-velocity is changed to

satisfy (6) and retain the same Jacobi's constant. The initial periodic orbit is blue and after each shift the color alternates between red and blue. The actual red and blue points are the locations on a particular orbit where (28) is satisfied. The curves on the y-axis are the maximum distance while the curves on the x-axis are the minimum distance. These red and blue curves show areas around Phobos where an orbit, with a particular Jacobi's constant, can be achieved and stay there. Similar results are shown for Deimos in Figure 6.

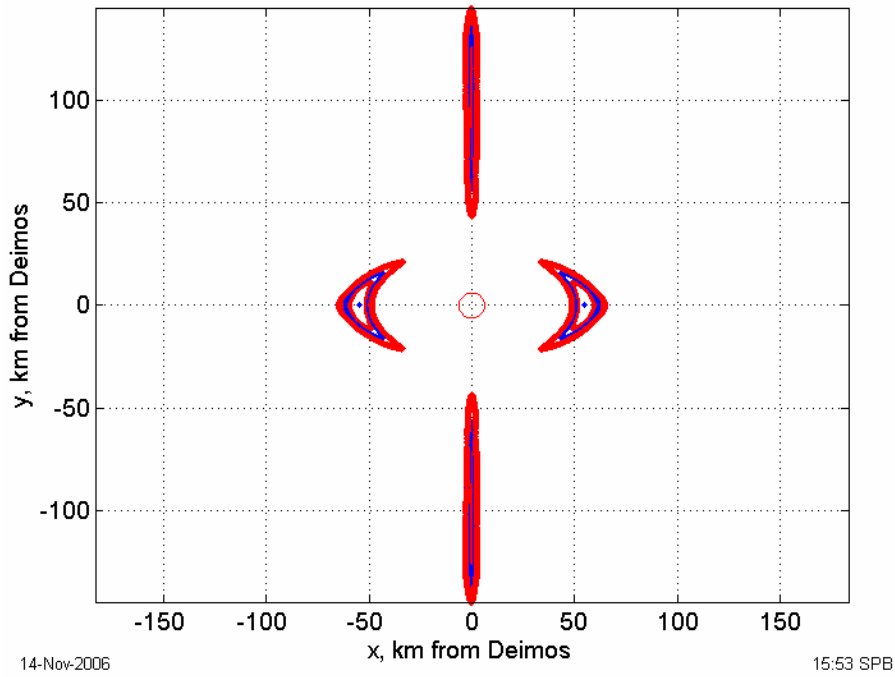


Figure 6a Surface of section for Deimos with $C = 2.999994501$

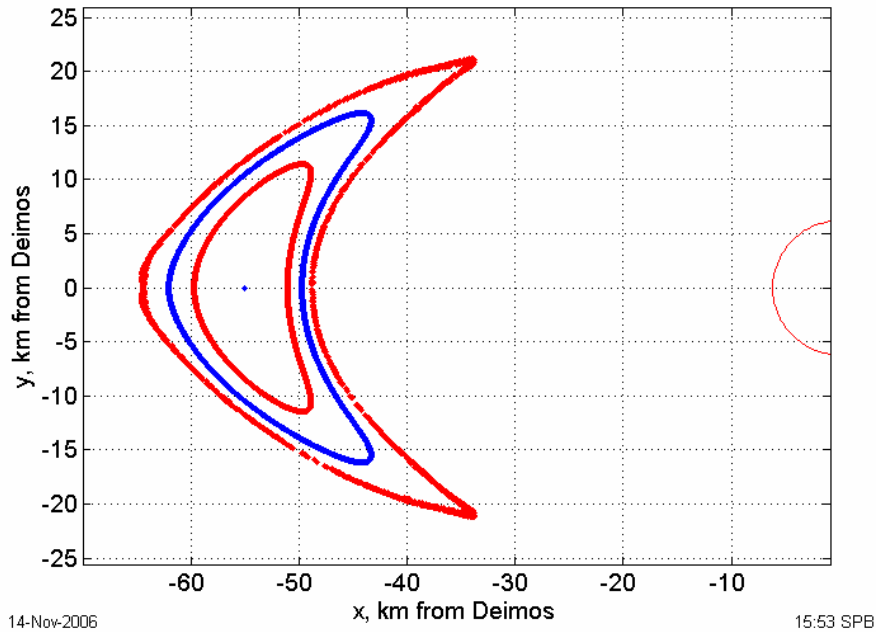


Figure 6b Enlarged view of left side of Figure 6a

As with Figure 5, Figure 6 shows four different orbits around Deimos that alternate from blue to red as they progress on x-axis from the blue periodic orbit at $r = 55$ km.

As earlier discussed, periodic orbits are found in the R3BP due to the EOM in (4) being invariant under the transformation t goes to $-t$ and y goes to $-y$. To determine whether or not similar periodic orbits exist when the EOM include spherical harmonic terms; the EOM first need to be analyzed under the transformation.

The EOM with spherical harmonic terms are not invariant under the transformation t goes to $-t$ and y goes to $-y$ when $m \neq 0$ because the longitude (10) changes sign and so the sine terms in (18-20) change sign since sine is an odd function. However, when $m=0$ these are zonals with no longitude variation and only the cosine terms are left in (18-20) and since cosine is an even function there is no sign change and the EOM are invariant. If the S_{nm} terms are ignored and only C_{nm} terms are used the EOM are invariant under the transformation. This analysis shows that similar periodic orbits are present for the EOM with C_{nm} harmonics only. Figures 7 and 8 on the next page show some periodic orbits at a few radii for both Phobos and Deimos with zonal harmonics only.

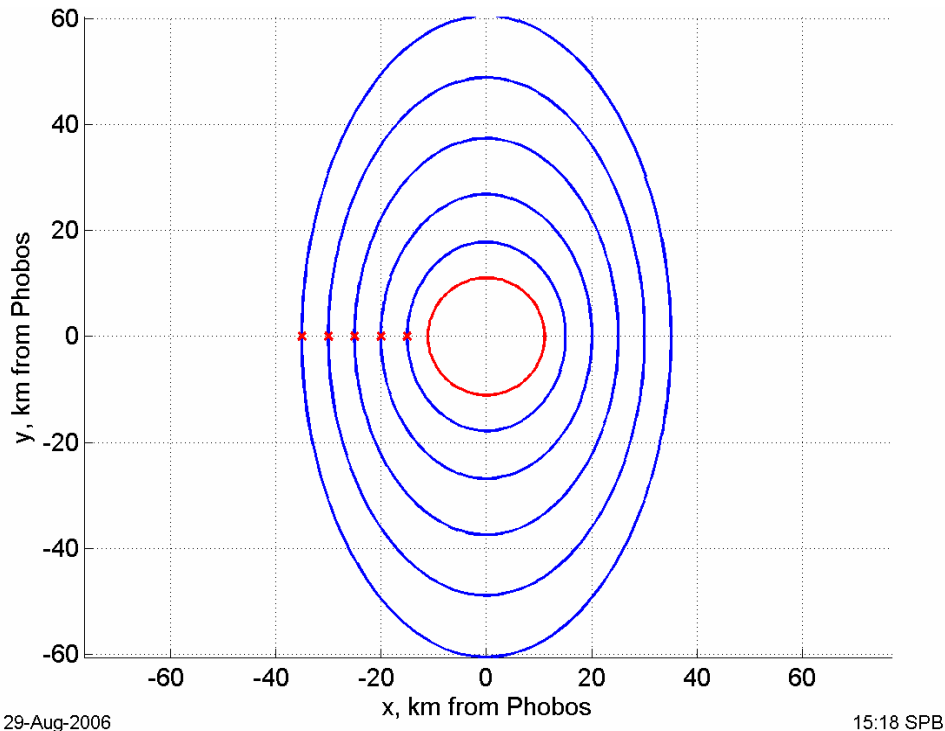


Figure 7 Periodic orbits for Phobos with zonal harmonics J2, J3 and J4

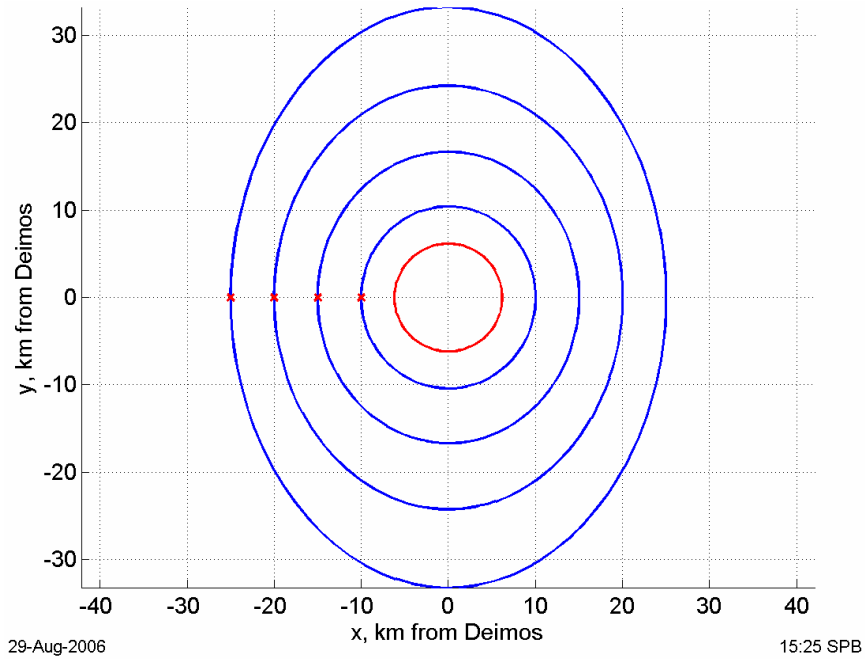


Figure 8 Periodic orbits for Deimos with zonal harmonics J2, J3, and J4

The next step in the study was to include all the C_{nm} terms but no S_{nm} terms in the model. The analysis performed earlier showing that the EOM are invariant when only C_{nm} terms are used will be tested. It was found that the orbits are periodic for both Phobos and Deimos, which is shown in Figures 9 and 10.

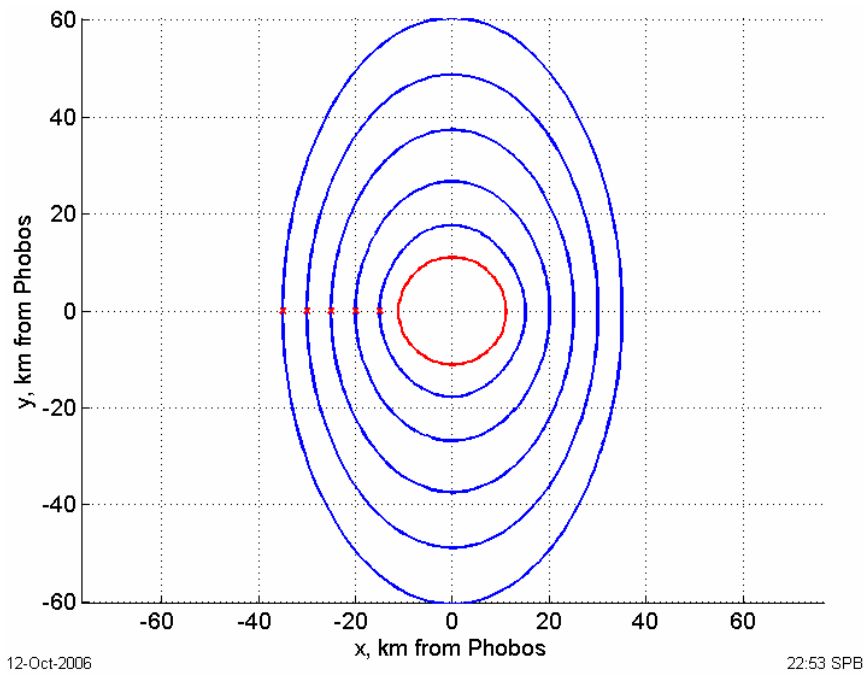


Figure 9 Periodic orbits for Phobos with only C_{nm} terms up to (4,4)

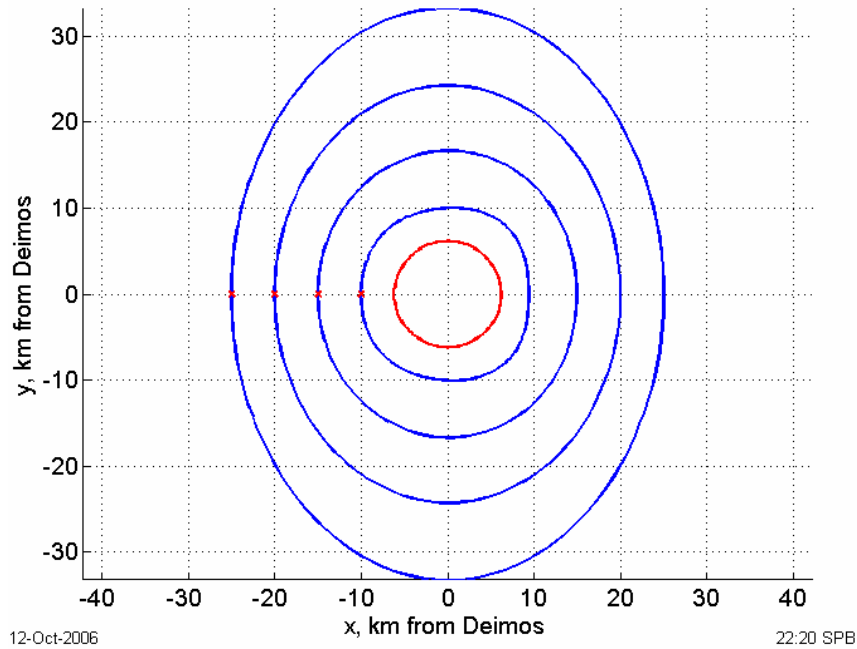


Figure 10 Periodic orbits for Deimos with only C_{nm} terms up to (4,4)

The final step in the study was to include the gravity fields of order and degree 4 for each of the moons. By including the higher order gravity terms the dynamics model will be more representative of the actual orbit behavior. It was found that including the higher order gravity terms the orbits had little change when at radii greater than 35 km, which is shown in Figure 11.

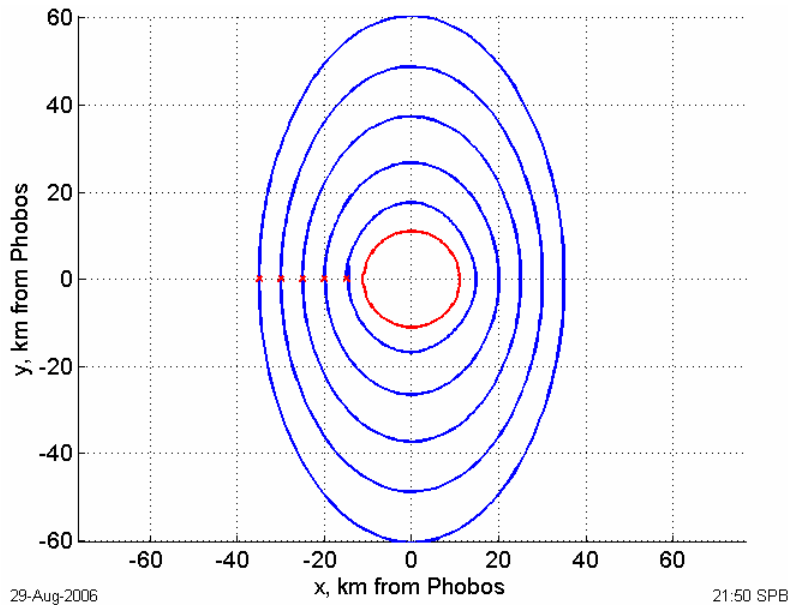


Figure 11a Orbits about Phobos including 4,4 gravity field

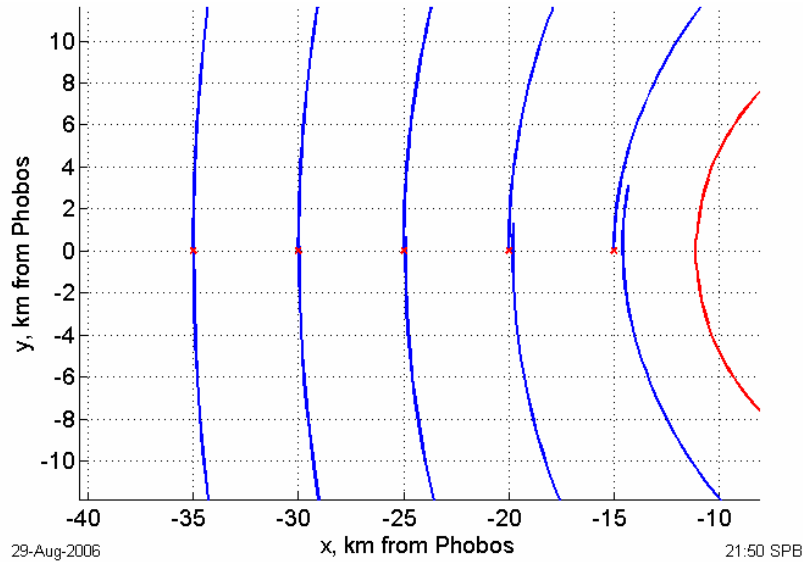


Figure 11b Enlarged view of left side of Figure 9a

The orbits in Figure 11 were found using the same method as the orbits in Figure 2, however as one can see in Figure 11b the orbits below $r = 35\text{km}$ are not periodic. None of these orbits are periodic; the difference is just easier to see below 35km . This result agrees with the analysis discussed earlier since including the S_{nm} terms both sine and cosine terms in (8) are involved, which destroys the symmetry needed to find the periodic orbits. The periodic orbits nearly return at greater distances because the particle will be dominated by the gravity of Mars and the higher order terms become negligible. The L_1 and L_2 locations for the Mars-Phobos system are approximately 16.5 km from the center of Phobos, which gives an indication of the influence of Mars gravity. Similar results are found for Deimos, which are shown in Figure 12.

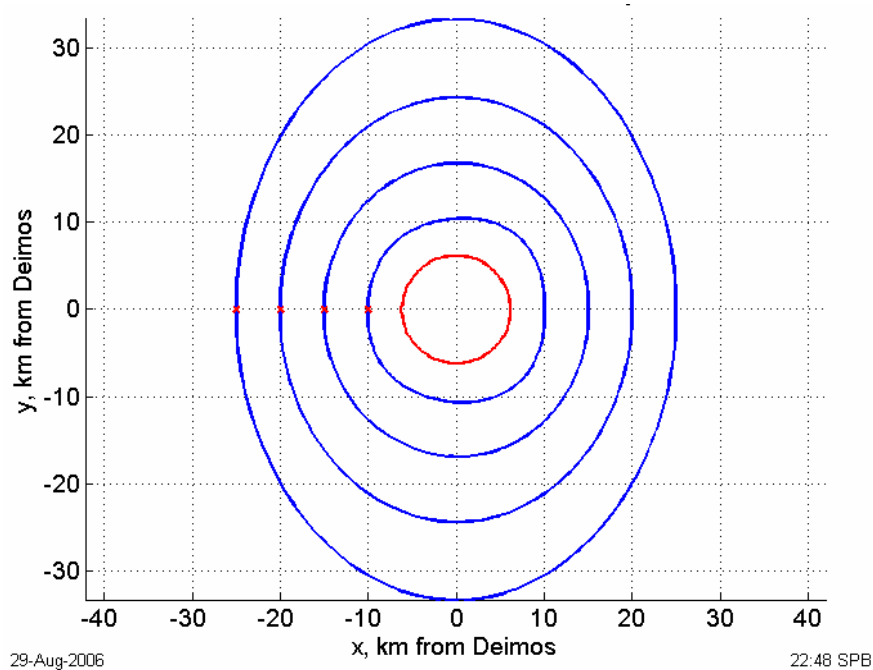


Figure 12a Orbits about Deimos including 4,4 gravity field

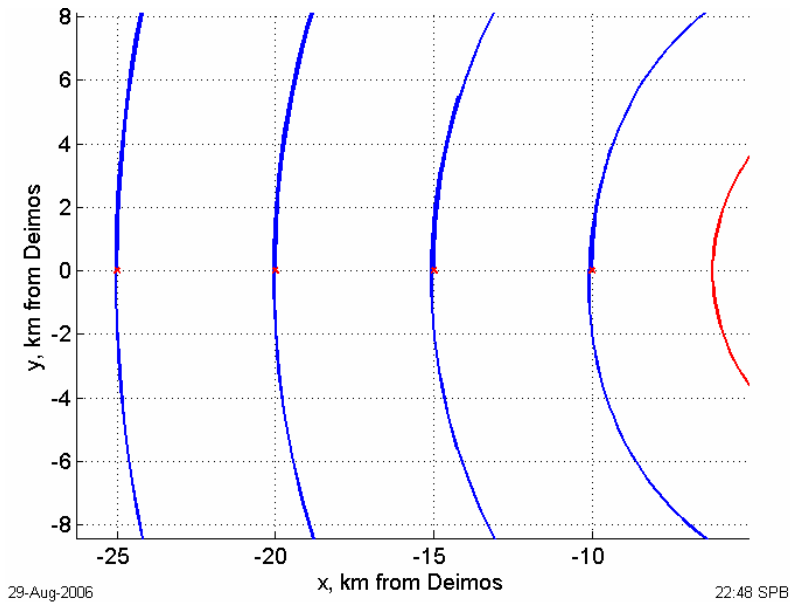


Figure 12b Enlarged view of left side of Figure 10a

In the case with Deimos, the periodic orbits nearly return at distances greater than $r = 25$ km. This result is due to the L_1 and L_2 locations of Mars-Deimos system being located approximately 21km from the center of Deimos and the large distance Deimos is from Mars. The nearly periodic orbits for Phobos and Deimos have essentially the same characteristics shown in Figure 4. However, the orbits closer to the moons are of more interest for both reconnaissance and for their convenient transfer to and from the surface. Some of these closer non-periodic orbits are shown in Figures 13 and 14.

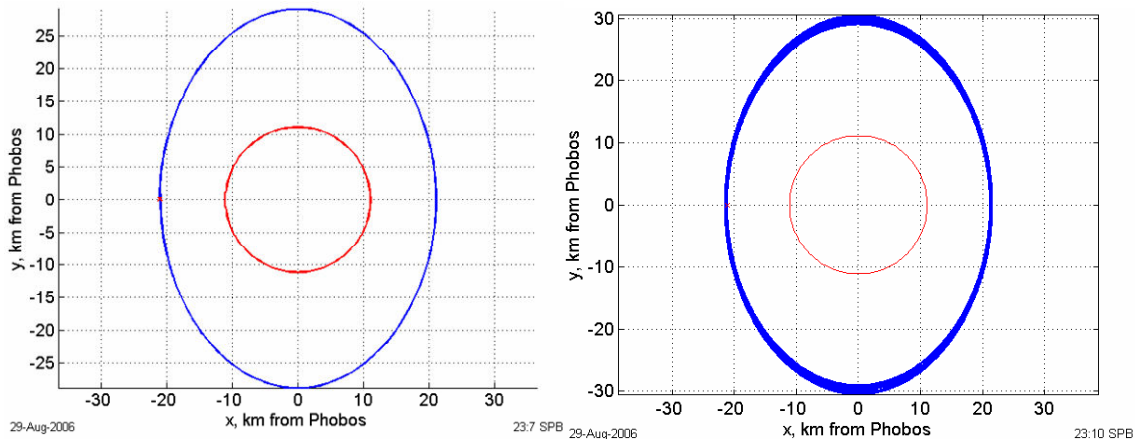


Figure 13 Quasi-periodic orbit about Phobos at 10km from surface (10 days, 57 orbits)

Figure 13 shows a possible parking orbit about Phobos with the 4,4 gravity field for one revolution (left) and a ten day span (right). Although this orbit is not periodic it has been shown to stay in the vicinity for at least ten days. Similar results are shown for Deimos in Figure 14.

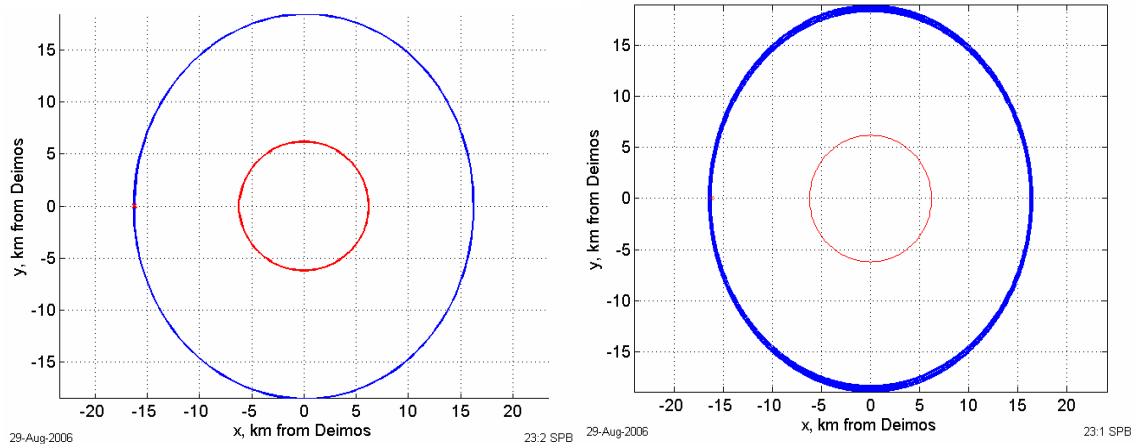


Figure 14 Quasi-periodic orbit about Deimos at 10km from surface (10 days, 26.5 orbits)

Figure 14 shows a possible parking orbit about Deimos with the 4,4 gravity field for one revolution (left) and a ten day span (right). The surface of section plots for the orbits in Figures 13 and 14 are shown in Figures 15 and 16.

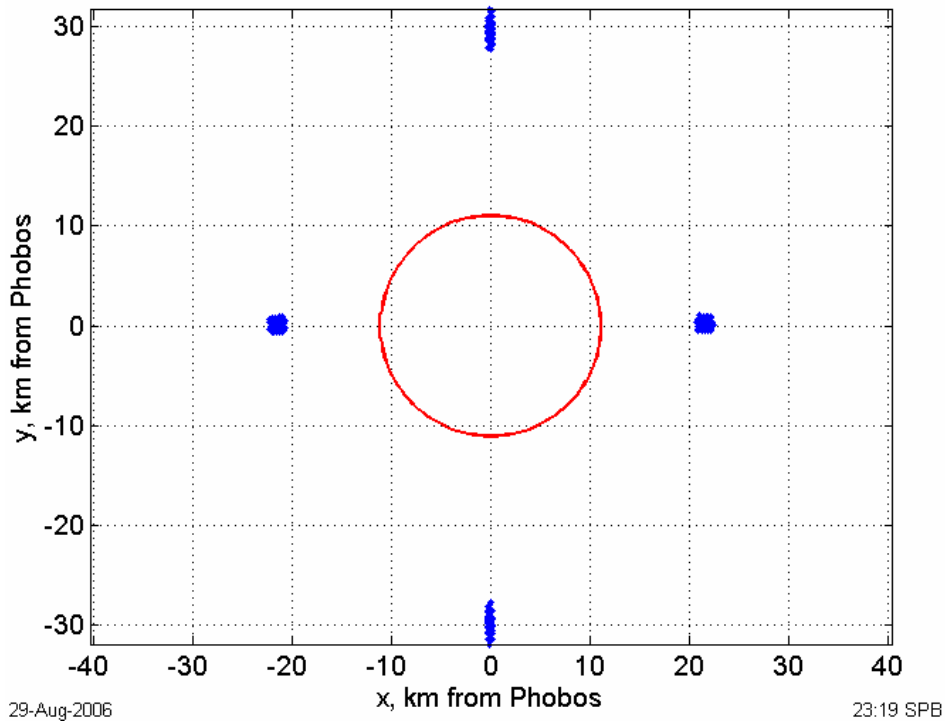


Figure 15 Surface of section for Phobos at $C = 2.99998321$ with 4,4 gravity field (10 days, 57.1 orbits)

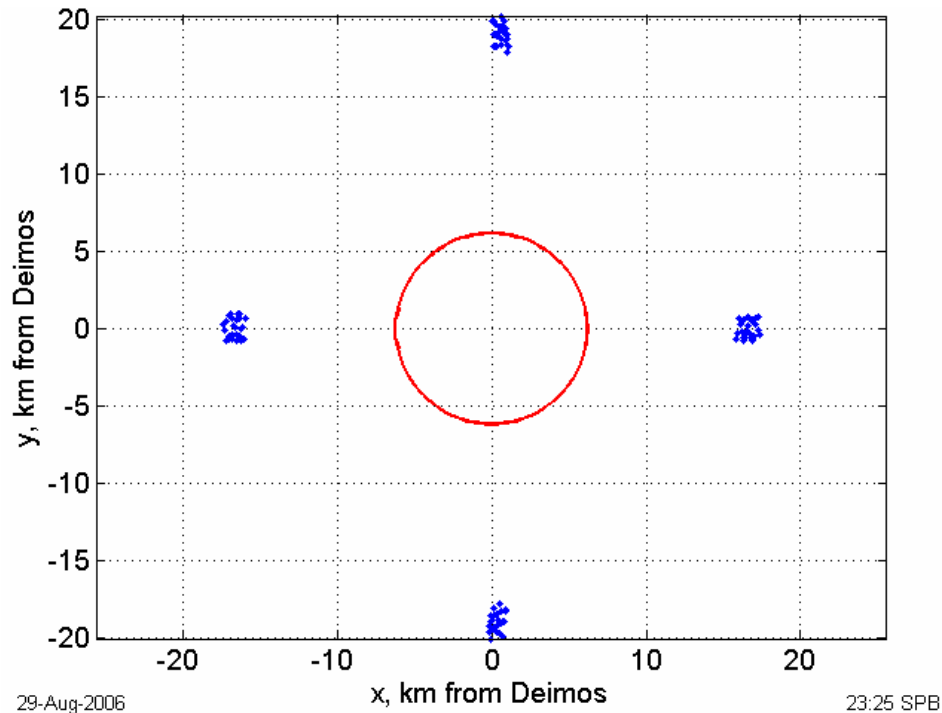


Figure 16 Surface of section for Deimos at $C = 2.99999426$ with 4,4 gravity field (10 days, 26.5 orbits)

The islands in both Figures 15 and 16 represent relative extremum of the corresponding orbits and they are for a single Jacobi's constant. One can see that the islands do not contain any closed curves, which does not necessarily indicate whether or not these orbits are unstable. These quasi-periodic parking orbits may be useful for a mission that would be interested in landing on the surface.

Conclusion and Recommendations

The nearly periodic orbits found for the moons at distances greater than $r = 35\text{km}$ would work well for staying in the moons vicinity for long periods of time. The orbits nearer to the moons appear to have little variation for at least ten days and may be useful for landing on the moons surface. With such low orbit velocities the δV for landing and returning to orbit should be less than 55 m/s each way for Phobos and less than 10 m/s each way for Deimos.

The studies in this paper should be expanded to include more perturbing affects such as the moons orbital eccentricities, higher order gravity terms for Mars, and solar perturbations. The first two recommendations have been published as mentioned in the introduction, however, they were not performed with the full 4,4 gravity field for each moon. These further studies would give an even more accurate depiction of the behavior for orbits about the moons of Mars.

References

1. Jansson, S. W., and Wiesel, W. E., "Orbiting a Rock: Stable Orbits about Phobos and Deimos," Proceedings of the AIAA/AAS Astrodynamics Conference (Portland, OR), AIAA, Washington DC, 1990, pp. 51-55 (AIAA Paper 90-2887)
2. Wiesel, W. E., "Stable Orbits About the Martian Moons," Journal of Guidance, Control, and Dynamics, Vol. 16, No. 3, May-June, 1993
3. Konopliv, A. S., Yoder, C. F., Standish, E. M., Yuan, D., and Sjogren, W. L., "A global solution for the Mars static and seasonal gravity, Mars orientation, Phobos and Deimos masses, and mars ephemeris," Icarus, Vol. 182, pp. 23-50, 2006
4. Thomas, P.C., "The Shape of Small Satellites," Icarus, Vol. 77, pp. 248-274, 1989
5. Jefferys, W. H., "An Atlas of Surface of Section for the Restricted Problem of Three Bodies," Publications of the Department of Astronomy, The University of Texas at Austin, Series II, Vol. 3, No. 6, 1971
6. Rubincam, D. P., Chao, B. F., and Thomas, P. C., "The Gravitational Field of Deimos," Icarus, Vol. 114, pp. 63-67, 1995
7. Rubincam, D. P., and Chao, B. F., "The Gravitational Field of Phobos," Geophysical Research Letters, Vol. 16, No. 8, pp. 859-862, 1989
8. Seidelmann, P. K., "Explanatory Supplement to the Astronomical Almanac," University Science Books, 1992
9. Szebehely, V., "Theory of Orbits," Academic Press Inc., New York, 1967
10. Shor, V. A., "The motions of the Martian satellites," Celestial Mechanics, Vol. 12, pp. 61-75, 1975
11. Dobrovolskis, A. R., and Burns, J. A., "Life Near the Roche Limit," Icarus, Vol. 42, pp. 422-441, 1980
12. Tolson, R. H., "Space Flight Mechanics and Space Flight Guidance and Navigation," North Carolina State University, Mechanical and Aerospace Engineering, 2006